

STINGLESS BEE HONEY INCORPORATED  
CELLULOSE HYDROGEL/POLY(LACTIC-CO-GLYCOLIC ACID) PATCH AS  
AN ALTERNATIVE TREATMENT FOR APHTHOUS STOMATITIS

ALEX ZHEN KAI LO,<sup>\*</sup> SITI KHADIJAH LUKMAN,<sup>\*</sup> CHIAN-HUI LAI,<sup>\*\*</sup>  
NORHIDAYU MUHAMAD ZAIN<sup>\*\*\*</sup> and SYAFIQA SAIDIN<sup>\*,\*\*\*\*</sup>

<sup>\*</sup>*School of Biomedical Engineering and Health Sciences, Faculty of Engineering, Universiti Teknologi Malaysia, 81310 UTM Johor Bahru, Johor, Malaysia*

<sup>\*\*</sup>*Graduate Institute of Biomedical Engineering, National Chung Hsing University, Taichung, Taiwan*

<sup>\*\*\*</sup>*Academy of Islamic Civilization, Faculty of Social Science and Humanities, Universiti Teknologi Malaysia, 81310 UTM Johor Bahru, Johor, Malaysia*

<sup>\*\*\*\*</sup>*IJN-UTM Cardiovascular Engineering Centre, Institute of Human Centered Engineering, Universiti Teknologi Malaysia, 81310 UTM Johor Bahru, Johor, Malaysia*

✉ *Corresponding author: S. Saidin, syafiqahsaidin@biomedical.utm.my*

Received May 28, 2020

Aphthous stomatitis is a disease that often reappears, causing irritation and pain. Common topical medications to treat aphthous stomatitis are fast-dissolving synthetic drugs, sometimes with limited therapeutic effectiveness. In this study, a patch, composed of a stingless bee honey incorporated cellulose hydrogel layer and a poly(lactic-co-glycolic acid) (PLGA) layer, was fabricated as an alternative treatment for aphthous stomatitis. The composition of the honey patches was verified by the presence of a distinct physical structure, considerable wettability records and lower degradation percentages on the layers containing higher PLGA concentrations. The honey patches were capable to retard *Escherichia coli* in the early hours (0.5-2 hours) and *Staphylococcus aureus* in the late hours (2-4 hours) of application, with tolerable cell viability and cell closure. The therapeutic values of the honey patches in retarding bacterial growth and inducing cell closure recommend the developed patches to be used in aphthous stomatitis treatment.

**Keywords:** stingless bee honey, patch, antibacterial, cell proliferation, aphthous stomatitis

## INTRODUCTION

Aphthous stomatitis, or recurrent aphthous stomatitis (RAS), is also known as mouth ulcer. It is the most common type of oral disease that occurs in the oral mucosa.<sup>1</sup> Aphthous stomatitis is a recurrent inflammatory lesion, which heals and reappears, causing irritation and pain to the patient.<sup>1,2</sup> According to the statistics, RAS has affected 5-25% of the general population.<sup>3</sup> Its appearance is due to various factors, including local trauma, bacterial infection, deficiency of nutrients, genetic factors and immune or endocrine disorders.<sup>4,5</sup>

Glucocorticoids, antibacterial agents and antiseptics, such as chlorhexidine, are the common drugs/materials to treat RAS, these medications being incorporated into topical pastes, mouthwashes and intralesional injections.<sup>3,6</sup> In spite of synthetic medications, natural-based ones,

such as honey, have been found effective in healing and preventing RAS.<sup>7</sup> Honey is one of the world's oldest foods, which also has medicinal functions of wound healing, as well as antibacterial, analgesic and anti-inflammatory effects.<sup>8-10</sup> It has the ability to stop bacterial growth due to its high sugar content, low pH and the presence of antibacterial factors, such as hydrogen peroxide.<sup>11</sup> There are several types of honey, its classification being based on the harvested region. In this study, stingless bee honey was chosen as the main therapeutic agent for RAS treatment due to its high antibacterial capacity.<sup>12</sup>

However, natural therapeutic medications incorporated into topical gels, creams and ointments are often washed away from the targeted lesion,<sup>6</sup> which reduces their efficiency for

RAS treatment. Hence, it would be more desirable to combine these natural-based medicines with sustainable carriers, such as hydrogels. In the past decades, hydrogels have attracted great attention in the field of biomedical materials, including drug delivery, cell therapy, wound healing, cartilage and bone regeneration.<sup>13</sup> Cellulose-based hydrogels have great potential due to low cost and availability of cellulose materials.<sup>14</sup> They are biocompatible, biodegradable, hydrophilic in nature and have strong mechanical strength depending on the source of the cellulose derivatives.<sup>15</sup> Cellulose hydrogels can be prepared by the utilisation of native cellulose, such as carboxymethyl cellulose (CMC), hydroxypropylmethyl cellulose (HPMC), cellulose acetate (CA), cellulose acetate phthalate (CAP) and bacterial cellulose.<sup>16</sup> Cavallari *et al.*<sup>17</sup> have developed mucoadhesive hydrogel patches made from SCMC and HPMC incorporated with chlorhexidine, while Songkro<sup>18</sup> have fabricated a bioadhesive nicotinamide oral gel, using SCMC and HPMC for oral mucosal lesion.

In this study, a cellulose hydrogel was used as a carrier to hold stingless bee honey for the purpose of therapeutic delivery. Sustainable therapeutic effects were projected due to the utilisation of poly(lactic-co-glycolic acid) (PLGA), another type of biodegradable polymer, which has been approved by the Food and Drug Administration.<sup>19</sup> Poly(lactic-co-glycolic acid) is prominent in the biomedical field and for dental applications due to its promising properties of biodegradability, biocompatibility and favourable release kinetics.<sup>20,21</sup> Therefore, stingless bee honey was incorporated into cellulose hydrogels, with layering of different PLGA concentrations, to sustain the desirable properties of the hydrogel. To the best of the authors' knowledge, no other study has been conducted so far on the layering of different PLGA concentrations in stingless bee honey incorporated cellulose hydrogels for RAS treatment. The honey patches were then subjected to physico-chemical characterisation, degradation, *in-vitro* antibacterial and *in-vitro* cell analyses to identify the mechanism performance, following the layering process.

## EXPERIMENTAL

### Sample preparation

Stingless bee honey (22% water content) was supplied by Bahtera Yubalam Enterprise, Malaysia. All the other materials were purchased from Sigma Aldrich, USA. A cellulose hydrogel without the

incorporation of stingless bee honey and without the PLGA layering was set as the control, while a cellulose hydrogel incorporating stingless bee honey, without PLGA layering, was denoted as HnH. The cellulose hydrogels incorporating stingless bee honey and with PLGA layering, were denoted as honey patches and referred to as *x*PLGA/HnH; where *x* = 0.01, 0.03, 0.05 and 0.07 g/mL PLGA, depending on the PLGA concentration.

The cellulose hydrogels were prepared by dissolving SCMC and HPMC in ethanol at 0.06 w/v%.<sup>17</sup> The mixture was heated up to 60 °C and stirred at 250 rpm using a magnetic stirrer, followed by the addition of polyethylene glycol 400 (PEG 400) and 70% distilled water. The weight ratio between the SCMC, HPMC and PEG 400 was set as 3:2:1. The mixture was continuously stirred for 30 minutes at 250 rpm, to allow hydrogel formation and solvent evaporation. The control hydrogel was then cast on a Petri dish and incubated for 2 days at 40 °C in an oven (UNB 300, Memmert, Germany), followed by storage at a temperature between 2 and 5 °C. For the fabrication of HnH, similar procedures were adopted, with an alteration in the content of distilled water from 70% to 40%. The 30% difference was covered by the addition of stingless bee honey into the cellulose mixture at room temperature, prior to the casting procedure in a Petri dish.

In the preparation of honey patches, the cellulose mixture incorporating stingless bee honey was prepared following similar procedures, without the casting phase. In another beaker, PLGA pellets with a lactide to glycolide ratio of 65:35 and molecular weight of 40,000-75,000 were dissolved in chloroform to form four different PLGA concentrations (0.01, 0.03, 0.05 and 0.07 g/mL). The solutions were layered individually in different Petri dishes to form PLGA layers and were set aside for 5 minutes. The cellulose hydrogel incorporating stingless bee honey, previously cooled to room temperature, was poured on the PLGA layers. The volume between the hydrogel and the PLGA solution was in a ratio of 20:1. The honey patches were finally incubated in an oven (UNB 300, Memmert, Germany) at 40 °C for 48 hours and stored in a refrigerator at 4 °C for 1 day, until further analyses.

### Sample characterisation

The chemical composition was analysed on both sides of the samples using attenuated total reflectance-Fourier transform infrared spectroscopy (ATR-FTIR, Spectrum Two, Perkin Elmer, USA). A diamond tip was used at a resolution of 4 cm<sup>-1</sup> to obtain the ATR-FTIR spectra. The spectra were recorded within the frequency range of 450-4000 cm<sup>-1</sup> at 32 average scans.

A bright-field microscope (Axio Vert A1, Carl Zeiss, Germany) was used to visualise the morphology of the samples under magnifications of 5× and 10×. The cross-section of the samples was also observed under an inverted microscope (OptikamB3, Optika,

Italy); the images were subjected to ImageJ (NIH, MD, USA) software for measuring layer thickness.

The wettability of the samples was then determined using a video contact angle instrument (Optima AST Product, Inc, USA) on both sides of the samples. An amount of 2  $\mu\text{L}$  of distilled water was dropped onto each surface at 1  $\mu\text{L/s}$ . The surface wettability was identified by calculating the average angle of the water droplet on three different spots.

#### Degradation test

The degradation of the samples was evaluated in phosphate buffer saline (PBS). The samples were cut to the dimensions of 10 mm  $\times$  10 mm and the initial weight of each sample was measured. The samples were then immersed separately in 5 mL of PBS and incubated in an incubator at 37  $^{\circ}\text{C}$  for 4 hours. After 4 hours, the samples were collected and dried for 6 hours at 40  $^{\circ}\text{C}$ . The dried samples were weighed again to obtain the final weight. The percentages of weight loss were calculated using Equation (1), where  $W_i$  is the initial weight of the sample and  $W_f$  is the final weight of the sample after the degradation test:

$$\text{Weight loss (\%)} = \frac{W_i - W_f}{W_i} \times 100\% \quad (1)$$

#### In-vitro antibacterial test

The antibacterial properties of the samples were verified with Gram-negative bacteria, *Escherichia coli* (*E. coli*), and Gram-positive bacteria, *Staphylococcus aureus* (*S. aureus*) through a bacterial count test. Prior to the antibacterial analyses, all apparatus and equipment were sterilised using an autoclave (HVE-50, Hirayama, Japan) at 120  $^{\circ}\text{C}$  for 30 minutes. The bacteria were cultured on Luria-Bertani (LB) nutrient agar and incubated overnight at 37  $^{\circ}\text{C}$ . A sterile inoculation loop was used to transfer a single bacterial colony to 100 mL of LB broth. The bacterial suspension was incubated overnight at 37  $^{\circ}\text{C}$  in a shaking incubator (SI-50D, Protech, Malaysia) at 180 rpm. The bacterial concentration was then adjusted to  $1 \times 10^8$  cells/mL using a spectrophotometer (Genesys 10S UV-Vis Spectrophotometer, Thermo Fisher Scientific Inc., USA).

The samples with the dimensions of 10 $\times$ 10 mm were immersed in 5 mL of bacterial suspension in centrifuge tubes. The centrifuge tubes were incubated separately at 37  $^{\circ}\text{C}$  for 0.5, 1, 2 and 4 hours in a shaking incubator, at 180 rpm. After the incubation, each bacterial suspension was diluted to eight dilution series. The drop plate method was used to grow the bacterial colonies, where 10  $\mu\text{L}$  of each dilution was dropped on nutrient agar and incubated at 37  $^{\circ}\text{C}$  overnight. The formed bacterial colonies were then counted manually to determine colony forming units (CFU) and to calculate bacterial reduction percentages, based on Equation (2):

$$\text{Bacterial reduction percentage (\%)} = \frac{\text{CFU}(\text{control}) - \text{CFU}(\text{sample})}{\text{CFU}(\text{control})} \times 100\%$$

#### In-vitro cell viability test

The biocompatibility of the samples was investigated with human skin fibroblast cells through the 3-(4,5-dimethylthiazol-2-yl)-2,5-diphenyl tetrazolium bromide (MTT) assay. A complete medium was prepared to culture the human skin fibroblast cells, which consisted of Gibco minimum essential medium (MEM), foetal bovine serum (FBS) and penicillin/streptomycin, in the ratio of 100:10:1. The extraction media were prepared by immersing the samples into the complete medium, independently, and incubated at 37  $^{\circ}\text{C}$  for 1 day.

The human skin fibroblast cells were then cultured in a 96-well cell culture plate at 37  $^{\circ}\text{C}$ , with a supplement of 5% carbon dioxide ( $\text{CO}_2$ ). The cell concentration was adjusted at  $1 \times 10^5$  cells/mL medium/well, with a confluency of 100%. The media were then replaced with 200  $\mu\text{L}$  of the extraction media and incubated for 1 day at 37  $^{\circ}\text{C}$ . After the incubation, the extraction media were removed and the cells were treated with 150  $\mu\text{L}$  of MTT solution, followed by continuous incubation for another 4 hours. Then, the MTT solution in each well was replaced with 150  $\mu\text{L}$  of dimethyl sulfoxide (DMSO). The observation of absorbance values at 540 nm was performed using a microplate reader (Thermo Scientific, Multiskan FC 51119000, Taiwan). The cell viabilities were then calculated using Equation (3):

$$\text{Cell viability (\%)} = \frac{\text{Optical density}(\text{test})}{\text{Optical density}(\text{control})} \times 100\% \quad (3)$$

#### In-vitro cell scratch test

The scratch test was then conducted to assess the ability of the samples to proliferate cells, imitating RAS closure. The human skin fibroblast cells ( $1 \times 10^5$  cells/1 mL medium/well) were cultured in a 24-well cell culture plate. After the cells reached 100% confluency, they were scratched using a sterile 200  $\mu\text{L}$  pipette tip. Each well was observed under a bright-field inverted fluorescence microscope (Carl Zeiss Axio Vert A1, USA) and the initial gap was captured and measured. The 24-well plate was then filled with 1 mL of the extraction medium and was incubated for 24 hours at 37  $^{\circ}\text{C}$  with 5%  $\text{CO}_2$ . After 24 hours, each well was observed again using the bright-field inverted microscope and the lengths of the closure gap were captured and measured. The measurements of the initial gap ( $G_i$ ) and of the final gap ( $G_f$ ) were done using ImageJ software (NIH, MD, USA). The gap closure percentages were finally calculated using Equation (4):

$$\text{Gap closure (\%)} = \frac{G_i - G_f}{G_i} \times 100\% \quad (4)$$

#### Statistical test

The data from the degradation and the *in-vitro* cell tests were subjected to statistical analysis by one-way analysis of variance (ANOVA), at  $p < 0.05$ , using GraphPad Prism software (v6.01, GraphPad Software Inc., California). Continuous post-hoc analysis by

Tukey's multiple comparison method was then used for further significance clarification.

## RESULTS AND DISCUSSION

### ATR-FTIR analysis

Figure 1 (a) shows the ATR-FTIR spectra recorded on the hydrogel surfaces of the samples. The broad band hydroxyl groups (O–H stretch) between the wavenumbers of 3200 and 3700  $\text{cm}^{-1}$  can be clearly seen in all the spectra, indicating the presence of water molecules in the hydrogels. The C–H, C–C and C–O stretching vibrations can be identified at 2850–3000  $\text{cm}^{-1}$ , 1638  $\text{cm}^{-1}$  and 966–1188  $\text{cm}^{-1}$ , respectively, testifying the composition of both the cellulose hydrogel<sup>22,23</sup> and the stingless bee honey. Meanwhile, the C=O groups, representing the ketone structure at 1759  $\text{cm}^{-1}$  and sugar compounds at 750–1500  $\text{cm}^{-1}$ , demonstrated the major components of honey.<sup>24,25</sup>

The ATR-FTIR spectra of the PLGA surfaces, with additional data on the pristine PLGA, without cellulose hydrogel (for comparison purpose), are shown in Figure 1 (b). The intensities of the hydroxyl group (O–H stretch) band were reduced and almost disappeared as the layers reflected more the character of PLGA, rather than the stingless bee honey. However, these peaks became more visible as the concentration of PLGA increased, in contrast with the theory of greater hydrophobicity with higher content of PLGA. It might be due to the interaction between the HnH (hydrophilic

material) and the PLGA layer (hydrophobic material), which contributed to the physical adsorption between those two materials.<sup>26</sup>

The chemical groups, which constituted the stingless bee honey and the cellulose hydrogel, such as C–H, C=O (ketone), C–O and C–C, were less identifiable. The honey patch with the lowest concentration of the PLGA layer (0.01PLGA/HnH) shows the imitation peaks of the HnH, instead of those of the pristine PLGA. Meanwhile, the PLGA fingerprint at the C=O stretch, representing the carboxylic acid of PLGA, was observed at 1742  $\text{cm}^{-1}$ . This peak was more prominent in the higher concentrations of PLGA.

### Morphology analysis

Figure 2 shows bright-field microscope images of the samples. A regular and clear surface was observed on the control, with the appearance of water gelation. Water gelation was less noticeable on the honey patches with higher concentrations of PLGA, also exhibiting the presence of air bubbles, represented by the dark spots in the images. Sample 0.01PLGA/HnH was remarked to have more air bubbles and an irregular surface, compared to the control and HnH. As the concentrations of PLGA increased, the surfaces became more irregular, with micropores and a distinct physical structure. This morphology plays an important role, providing contact guidance for cell attachment.<sup>27</sup>

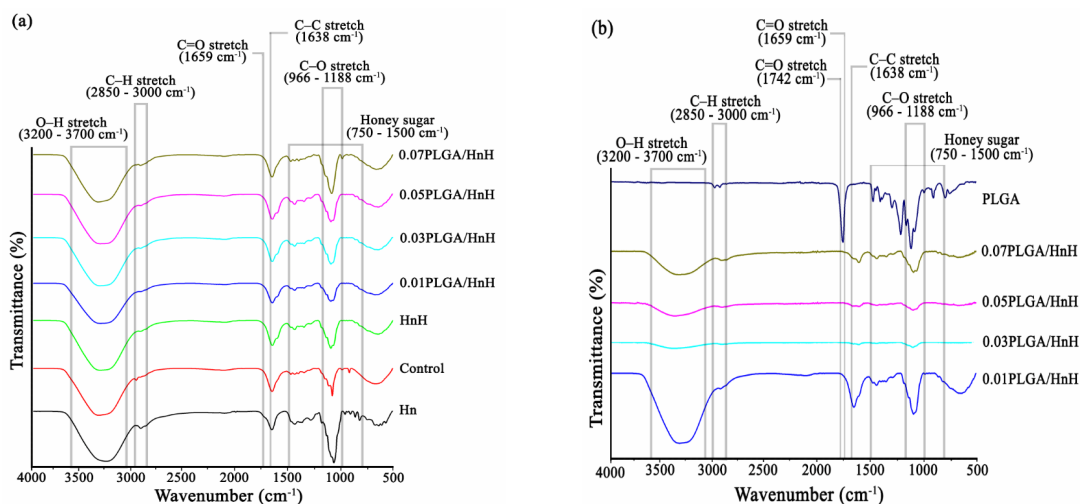


Figure 1: ATR-FTIR spectra of stingless bee honey (Hn), cellulose hydrogel (control), cellulose hydrogel with incorporated stingless bee honey (HnH) and honey patches with different PLGA concentrations ( $x$ PLGA/HnH;  $x = 0.01, 0.03, 0.05$  and  $0.07$ ) on the surfaces of (a) hydrogel and (b) PLGA

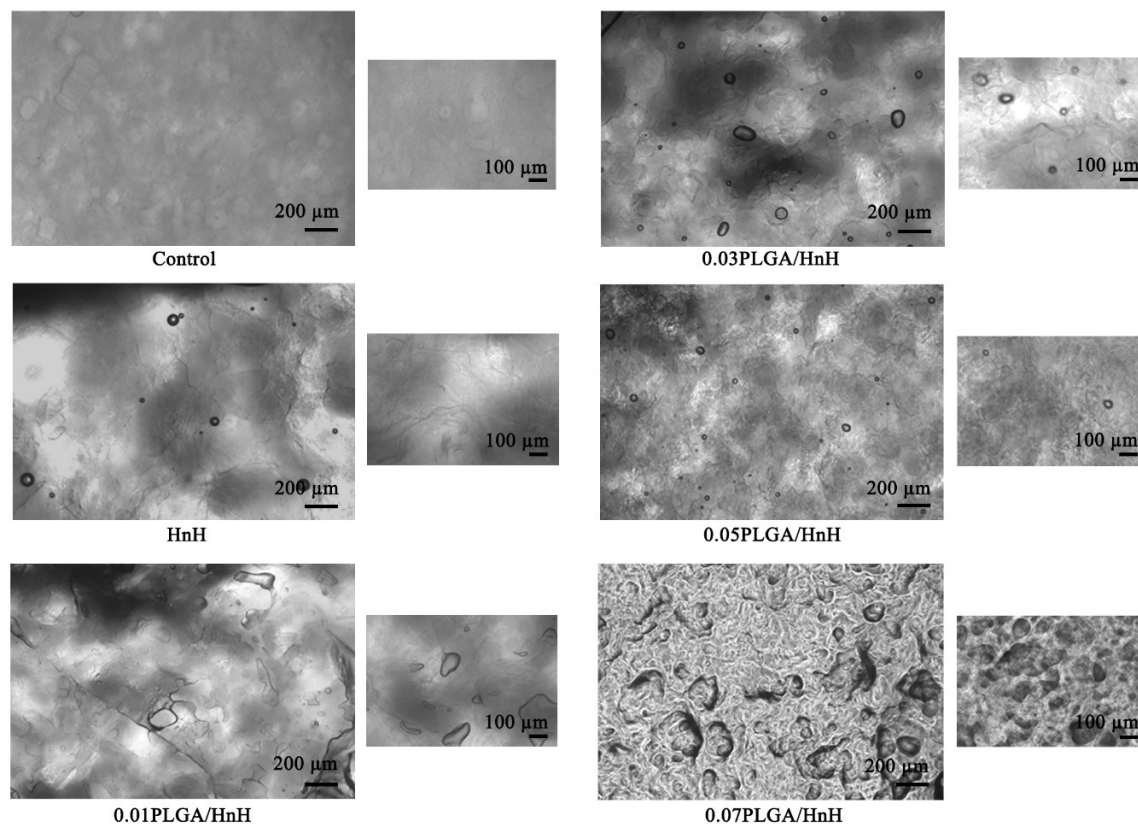


Figure 2: Morphology of cellulose hydrogel (control), cellulose hydrogel with incorporated stingless bee honey (HnH) and honey patches with different PLGA concentrations ( $x$ PLGA/HnH;  $x = 0.01, 0.03, 0.05$  and  $0.07$ )

The PLGA was seen in the form of a layer at the bottom of the stingless bee honey cellulose hydrogels, constructing the double layer polymeric materials, as viewed in Figure 3. Sample 0.01PLGA/HnH has an overall thickness of  $1.754 \pm 0.035$  mm, with  $0.095 \pm 0.003$  mm PLGA (alone) thickness. Sample 0.03PLGA/HnH has an overall thickness of  $1.710 \pm 0.013$  mm, with  $0.117 \pm 0.003$  mm PLGA (alone) thickness. For samples 0.05PLGA/HnH and 0.07PLGA/HnH, the overall thickness of  $1.767 \pm 0.023$  mm and  $1.783 \pm 0.047$  mm was recorded, respectively, with  $0.153 \pm 0.006$  mm and  $0.205 \pm 0.005$  mm PLGA (alone) thickness, respectively. The overall thickness of the honey patches did not differ apparently due to the similar environment conditions during the fabrication process. However, the PLGA thickness showed an increasing trend, associated with PLGA viscosity.

#### Water contact angle analysis

As the honey patches are intended for the application on oral lesions, it is necessary to identify their wettability properties. Therefore, the water contact angle data recorded on the surface of cellulose hydrogels and PLGA layers are listed in Table 1. The wettability properties were reduced on the honey patches in comparison with the control and HnH, which led to an increment in the water contact angle values. On the surface of the PLGA layers, a decrement in wettability properties was noticed as the concentrations of PLGA increased, the samples thus approaching the hydrophobicity of the pristine PLGA. However, the honey patches were still considered hydrophilic due to the contact angle records of lower than  $90^\circ$ ,<sup>28</sup> which is important in forecasting preferable cell adhesion on the surfaces.<sup>29</sup>

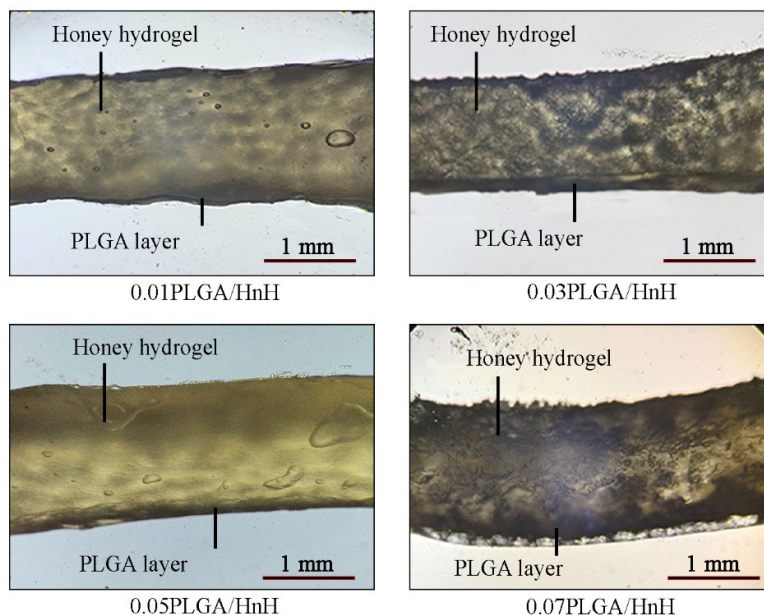


Figure 3: Cross-section images of honey patches with different PLGA concentrations ( $x$ PLGA/HnH;  $x = 0.01, 0.03, 0.05$  and  $0.07$ )

Table 1

Wettability records on cellulose hydrogel (control), cellulose hydrogel with incorporated stingless bee honey (HnH) and honey patches with different PLGA concentrations ( $x$ PLGA/HnH;  $x = 0.01, 0.03, 0.05$  and  $0.07$ )

Sample	Contact angle	
	Cellulose hydrogel layer	PLGA layer
Control	$54.23 \pm 0.31^\circ$	-
HnH	$53.83 \pm 0.37^\circ$	-
0.01PLGA/HnH	$62.30 \pm 3.11^\circ$	$63.40 \pm 0.60^\circ$
0.03PLGA/HnH	$65.06 \pm 3.40^\circ$	$65.40 \pm 0.98^\circ$
0.05PLGA/HnH	$64.73 \pm 1.15^\circ$	$67.50 \pm 0.34^\circ$
0.07PLGA/HnH	$50.73 \pm 4.59^\circ$	$69.00 \pm 0.20^\circ$
PLGA	-	$74.97 \pm 1.76^\circ$

### Degradation analysis

Figure 4 shows the degradation percentages of the cellulose hydrogel (control), the cellulose hydrogel with incorporated stingless bee honey (HnH) and the honey patches at different concentrations of PLGA ( $x$ PLGA/HnH;  $x = 0.01, 0.03, 0.05$  and  $0.07$ ), after immersion into PBS for 4 hours at  $37^\circ\text{C}$ . The control possessed  $48.11 \pm 1.62\%$  degradation percentage, with no significant difference from the degradation percentage of HnH,  $51.64 \pm 2.75\%$ . Sample 0.01PLGA/HnH was observed to have  $36.94 \pm 1.46\%$  degradation percentage, while for 0.03PLGA/HnH, 0.05PLGA/HnH and 0.07PLGA/HnH, the degradation percentages were found to be  $33.35 \pm 1.50\%$ ,  $26.56 \pm 1.86\%$  and  $23.37 \pm 2.83\%$ , respectively. The degradation

percentages for the honey patches differed significantly, except those of 0.01PLGA/HnH and 0.03PLGA/HnH, as well as those of 0.05PLGA/HnH and 0.07PLGA/HnH.

The introduction of PLGA layers into the honey patches ( $x$ PLGA/HnH) has decreased the degradation percentages significantly, compared to the control and HnH. The hydrophobic PLGA has influenced the dissolvability of the honey patches,<sup>30</sup> thus controlling their degradation behaviour.<sup>31</sup> The physical adsorption between HnH and PLGA also contributed to the reduction of degradation percentages due to the bonds that hold those two layers together.<sup>26</sup>

### Antibacterial analyses

Bacterial infection is one of the factors causing the appearance of RAS.<sup>4,6</sup> There is a necessity to utilise antibacterial agents, for example honey, in the fabrication of oral patches to control bacterial growth on RAS lesions. Therefore, Gram-negative *E. coli* and Gram-positive *S. aureus* were used to clarify the antibacterial properties of the honey patches developed in this study. The bacterial reduction percentages of *E. coli* for all the samples are shown in Figure 5 (a). The control hydrogel, without stingless bee honey, inhibited approximately 10% of *E. coli* growth in a sustained pattern up to 4 hours. The incorporation of stingless bee honey into the matrix of the cellulose hydrogels (HnH) caused an over 2-fold increment in bacterial reduction percentages up to 1 hour. The percentages dropped drastically after 2 hours of incubation to  $10.98 \pm 0.833\%$  and increased back to  $16.22 \pm 0.01\%$ , showing the burst release of honey.

The honey patches 0.01PLGA/HnH and 0.03PLGA/HnH have a similar pattern of antibacterial inhibition, as the highest bacterial reduction percentages were attained at 0.5 hour incubation, with  $34.15 \pm 0.50\%$  and  $39.02 \pm 3.58\%$ , respectively. The stingless bee honey was then gradually released, as the minimum percentages were obtained at 4 hours incubation, with  $5.41 \pm 0.02\%$  and  $6.76 \pm 0.60\%$ , respectively. As the concentrations of PLGA increased, the bacterial growth was retarded at the later incubation time

point, where the patch 0.05PLGA/HnH showed the greatest inhibition at 1 hour incubation ( $26.66 \pm 2.79\%$ ), while the patch 0.07PLGA/HnH had the highest inhibition at 2 hours incubation ( $26.83 \pm 0.08\%$ ).

Figure 5 (b) presents the bacterial reduction percentages using *S. aureus*. The control hydrogels have low capability in retarding bacterial growth, with less than 10% reduction. The addition of stingless bee honey into the hydrogels led to an increment in the reduction percentages to  $60.04 \pm 0.53\%$  at 4 hours incubation. 0.01PLGA/HnH and 0.03PLGA/HnH demonstrated similar inhibition patterns, as PLGA controlled the release of honey up to the maximum incubation time point with  $58.37 \pm 0.85\%$  and  $47.13 \pm 0.11\%$ , respectively. Different patterns of bacterial retardation were observed for 0.05PLGA/HnH, with the highest bacterial reduction of  $44.73 \pm 0.16\%$  at 2 hours incubation, and the maximum bacterial reduction of  $75.60 \pm 0.71\%$  was seen for 0.07PLGA/HnH at 4 hours incubation. The physical adsorption between HnH and PLGA became stronger on the higher PLGA concentration layers, which controlled the release of HnH. Another interaction between the hydrophobic and hydrophilic materials caused stronger repulsion<sup>32</sup> at the higher PLGA concentrations, which repelled the HnH molecules from the honey patches in a greater amount.

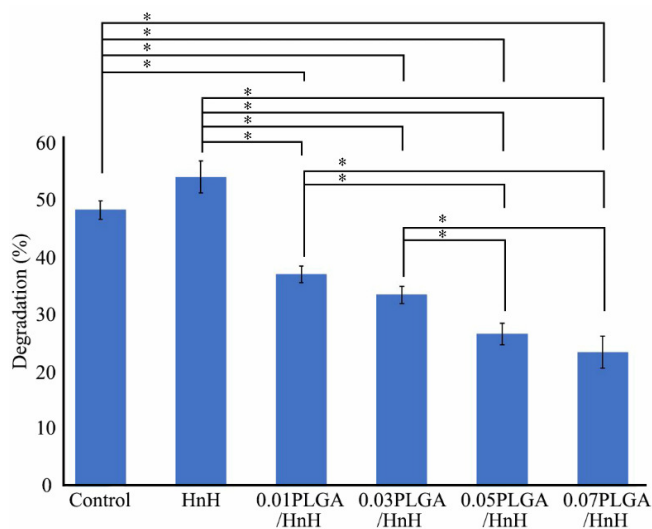


Figure 4: Degradation percentages of cellulose hydrogel (control), cellulose hydrogel with incorporated stingless bee honey (HnH) and honey patches with different PLGA concentrations ( $x$ PLGA/HnH;  $x = 0.01, 0.03, 0.05$  and  $0.07$ ) after 4 hours of immersion

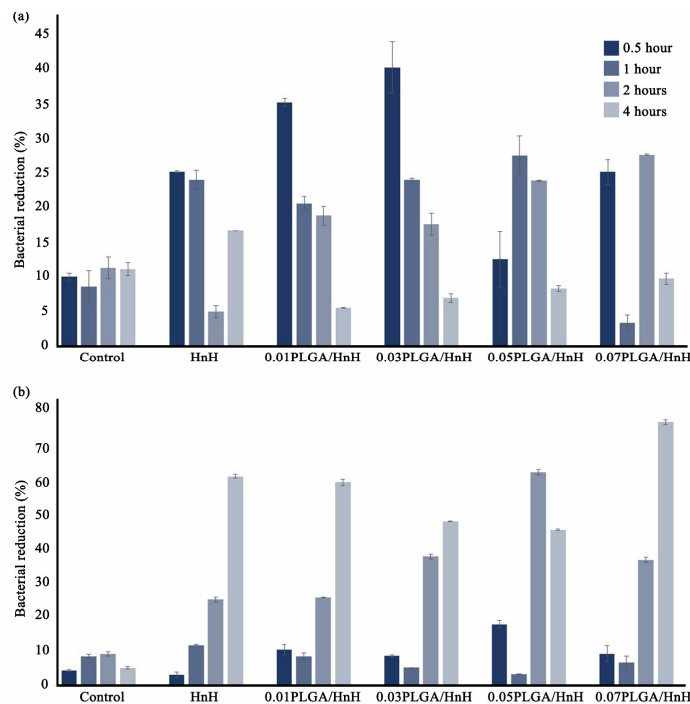


Figure 5: Bacterial reduction percentages recorded for cellulose hydrogel (control), cellulose hydrogel with incorporated stingless bee honey (HnH) and honey patches with different PLGA concentrations ( $x$ PLGA/HnH;  $x = 0.01, 0.03, 0.05$  and  $0.07$ ), at four different time points on (a) *E. coli* and (b) *S. aureus*

The combination of the data on *E. coli* and *S. aureus* showed that the honey patches were able to retard the growth of Gram-negative *E. coli* in the first 2 hours, but continued to inhibit Gram-positive *S. aureus* in the next 2 hours. The antibacterial activities produced by HnH and the honey patches were due to the stingless bee honey. The antibacterial properties of stingless bee honey are mainly due to its peroxide and non-peroxide activities.<sup>33</sup> The peroxide activity refers to the activity of hydrogen peroxide in the stingless bee honey, produced by glucose oxidase. The saturation of hydrogen peroxide will initiate cytokine secretion, thus triggering an inflammatory response in killing the bacteria.<sup>33</sup>

Besides the peroxide activity, the non-peroxide activity also plays an important role in the antibacterial mechanism of stingless bee honey. The non-peroxide activity refers to the non-peroxide composition of chemical components, high sugar content and honey acidity.<sup>33</sup> Flavonoids, phenolic compounds and antibacterial peptides are among the chemical components in stingless bee honey that are responsible for its antibacterial capability,<sup>34</sup> while the high sugar

content will create osmotic pressure, dragging water molecules out of the bacteria, thus initiating bacterial dehydration. Another factor is honey acidity, which is associated with the creation of an environment that is not suitable for bacterial growth, as bacteria require an environmental pH ranging from 7.2-7.4 to maintain their growth profile.<sup>35</sup>

#### ***In-vitro* cell viability analysis**

All the samples were verified in terms of their biocompatibility with human skin fibroblast cells. The results in Figure 6 show high cell viabilities for all the samples, *i.e.* more than 90%. The cells exposed to the control hydrogels produced a viability of  $94.24 \pm 9.57\%$ . The viability percentages increased to the maximum of  $218.35 \pm 7.80\%$  for the honey patches at 0.01 g/mL of PLGA. Increasing the PLGA concentrations to more than 0.01 g/mL of PLGA projected a reduction in cell viabilities, whereas the honey patch at 0.05 g/mL PLGA produced insignificant data, compared to the honey hydrogels, while the honey patch at 0.07 g/mL of PLGA showed insignificant data compared to the control.



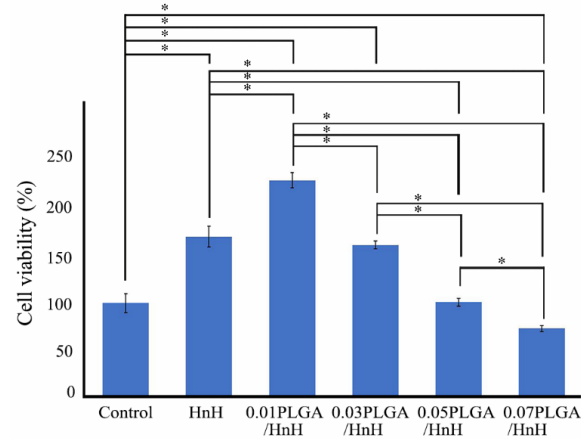


Figure 6: Cell viability data for cellulose hydrogel (control), cellulose hydrogel with incorporated stingless bee honey (HnH) and honey patches with different PLGA concentrations ( $x$ PLGA/HnH;  $x = 0.01, 0.03, 0.05$  and  $0.07$ )

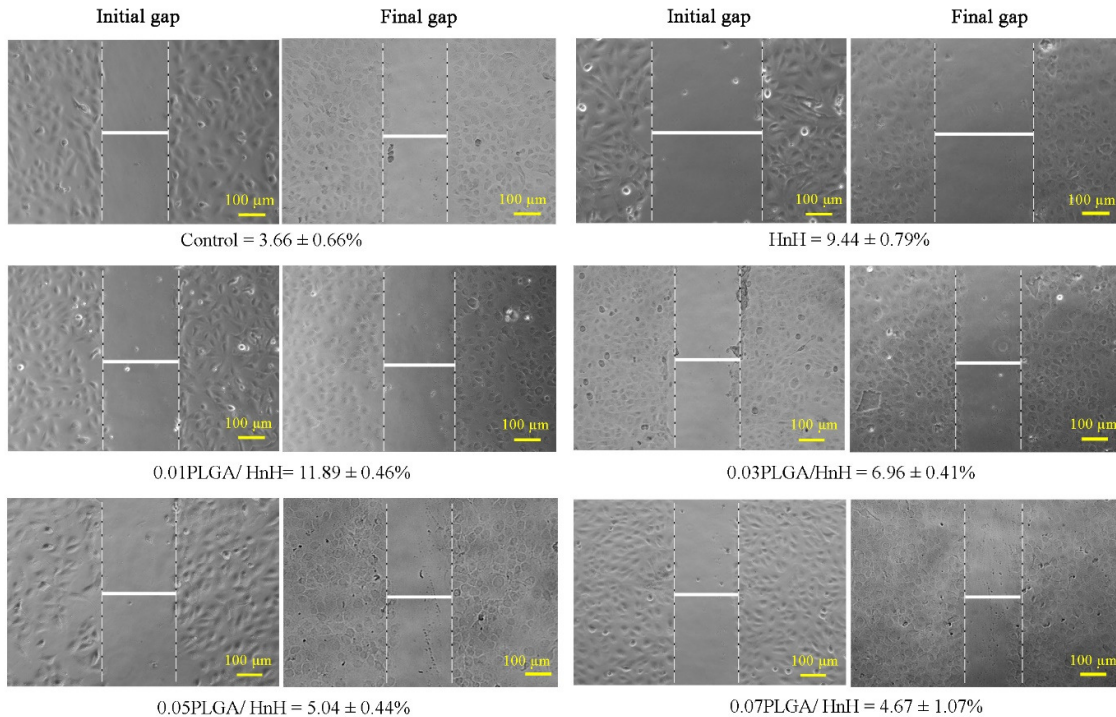


Figure 7: Microscopy images of initial and final cell gap closure for cellulose hydrogel (control), cellulose hydrogel with incorporated stingless bee honey (HnH) and honey patches with different PLGA concentrations ( $x$ PLGA/HnH;  $x = 0.01, 0.03, 0.05$  and  $0.07$ ), following 24 hours of incubation

### ***In-vitro* cell scratch analysis**

The ability of the samples to accelerate cell proliferation is revealed through the cell scratch analysis. Figure 7 shows the percentages of cell gap closure when the human skin fibroblast cells were exposed to the samples for 24 hours. The control projected the minimum closure percentage, of  $3.66 \pm 0.66\%$ . The HnH induced a closure

percentage approaching the 3-fold value of the control. This is due to the remarkable properties of stingless bee honey, which can promote angiogenesis by supporting tissue granulation and skin re-epithelialisation, which are favourable for wound healing acceleration.<sup>34</sup> These results also support the capability of PLGA to release the stingless bee honey into the extracellular matrix,

while 0.01PLGA/HnH has proliferated the cells and closed the cell gap more rapidly than HnH. Increasing the concentrations of PLGA did not favour the closure percentages, as significant reductions were found on the honey patches of 0.03PLGA/HnH, 0.05PLGA/HnH and 0.07PLGA/HnH. These results are in accordance with the results of cell viability.

Natural honey exhibits various nutritional qualities that are highly effective against reactive oxygen species (ROS), inflammation, infectious agents and possess wound curing characteristics.<sup>36</sup> The incorporation of stingless bee honey into the cellulose hydrogels (HnH) revealed a significant cell proliferation trend, due to the properties of stingless bee honey. As stated by Yaghoobi *et al.*,<sup>37</sup> honey can induce the proliferation of fibroblast cells and epithelial cells, whereas cell proliferation is one of the important phases in lesion healing, triggered by the growth factor, cytokines and other components.<sup>38</sup> The production of cytokines by cells (keratinocytes, macrophages and leukocytes) that are involved in lesion healing can be enhanced by the presence of stingless bee honey due to the production of hydrogen peroxide from the glucose oxidation.<sup>39</sup> Therefore, in this study, the utilisation of stingless bee honey in the honey patches has not only demonstrated non-toxicity, but also assisted cell proliferation.

## CONCLUSION

The fabrication of honey patches in this study is specifically intended to treat RAS. The cellulose hydrogel was cast to be the matrix carrier for the delivery of stingless bee honey. The layering of different concentrations of PLGA, ranging from 0.01 to 0.07 g/mL, played a role in controlling the therapeutic effects of honey, as a medium for cell differentiation and proliferation, while providing an antibacterial effect. The honey patches at 0.01 to 0.03 g/mL have delivered sustainable antibacterial effects, with maximum fibroblast cell viability and cell gap closure.

**ACKNOWLEDGMENT:** This study was supported by the Research University Grant (RUG) Tier 1 [Q.J130000.2545.18H40], provided by the Ministry of Education, Malaysia.

## REFERENCES

<sup>1</sup> R. Z. Cui, A. J. Bruce and R. S. Rogers, *Clin. Dermatol.*, **34**, 475 (2016), <https://doi.org/10.1016/j.clinidematol.2016.02.020>

<sup>2</sup> Y. Rajmane, S. Ashwinirani, G. Suragimath, A. Nayak, V. Rajmane *et al.*, *J. Oral Res. Rev.*, **9**, 25 (2017), [https://doi.org/10.4103/jorr.jorr\\_33\\_16](https://doi.org/10.4103/jorr.jorr_33_16)

<sup>3</sup> I. Belenguer-Guallar, Y. Jiménez-Soriano and A. Claramunt-Lozano, *J. Clin. Exp. Dent.*, **6**, e168 (2014), <https://doi.org/10.4317/jced.51401>

<sup>4</sup> N. R. Edgar, D. Saleh and R. A. Miller, *J. Clin. Aesthet. Dermatol.*, **10**, 26 (2017), [https://www.ncbi.nlm.nih.gov/pmc/articles/PMC5367879/pdf/jcad\\_10\\_3\\_26.pdf](https://www.ncbi.nlm.nih.gov/pmc/articles/PMC5367879/pdf/jcad_10_3_26.pdf)

<sup>5</sup> S. M. Gondivkar, A. R. Gadail, R. S. Gondivkar, S. C. Sarode, G. S. Sarode *et al.*, *Dis. Mon.*, **65**, 147 (2019), <https://doi.org/10.1016/j.disamonth.2018.09.009>

<sup>6</sup> B. Tarakji, G. Gazal, S. A. Al-Maweri, S. N. Azzeghaiby and N. Alaizari, *J. Int. Oral Health*, **7**, 74 (2015), <https://www.ncbi.nlm.nih.gov/pmc/articles/PMC4441245/pdf/JIOH-7-74.pdf>

<sup>7</sup> S. A. El-Haddad, F. Y. L. Asiri, H. H. Al-Qahtani and A. S. Al-Ghmlas, *Quintessence Int.*, **45**, 691 (2014), <https://doi.org/10.3290/j.qi.a32241>

<sup>8</sup> S. Rao, S. Hegde, P. Rao, C. Dinkar, K. Thilakchand *et al.*, *Foods*, **6**, 77 (2017), <https://doi.org/10.3390/foods6090077>

<sup>9</sup> S. Ahmed and N. H. Othman, *Malays. J. Med. Sci.*, **20**, 6 (2013), <https://www.ncbi.nlm.nih.gov/pmc/articles/PMC3743976/pdf/mjms-20-3-006.pdf>

<sup>10</sup> F. F. Abd El-Malek, A. S. Yousef and S. A. El-Assar, *J. Glob. Antimicrob. Resist.*, **11**, 171 (2017), <https://doi.org/10.1016/j.jgar.2017.08.007>

<sup>11</sup> E. I. Ramsay, S. Rao, L. Madathil, S. K. Hegde, M. P. Baliga-Rao *et al.*, *J. Oral Biosci.*, **61**, 32 (2019), <https://doi.org/10.1016/j.job.2018.12.003>

<sup>12</sup> M. I. Zainol, K. Mohd Yusoff and M. Y. Mohd Yusof, *BMC Complem. Altern. M.*, **13**, 129 (2013), <https://doi.org/10.1186/1472-6882-13-129>

<sup>13</sup> N. Chirani, L. H. Yahia, L. Gritsch, F. Motta, S. Chirani *et al.*, *J. Biomed. Sci.*, **4**, 13 (2015), <https://doi.org/10.4172/2254-609X.100013>

<sup>14</sup> X. Shen, J. Shamshina, P. Berton, D. Gurau and R. D. Rogers, *Green Chem.*, **18**, 53 (2015), <https://doi.org/10.1039/C5GC02396C>

<sup>15</sup> C. Chang and L. Zhang, *Carbohydr. Polym.*, **84**, 40 (2011), <https://doi.org/10.1016/j.carbpol.2010.12.023>

<sup>16</sup> S. M. F. Kabir, P. P. Sikdar, B. Haque, M. A. Rahman Bhuiyan and M. N. Islam, *Progr. Biomater.*, **7**, 153 (2018), <https://doi.org/10.1007/s40204-018-0095-0>

<sup>17</sup> C. Cavallari, P. Brigidi and A. Fini, *Int. J. Pharm.*, **496**, 593 (2015), <https://doi.org/10.1016/j.ijpharm.2015.10.077>

<sup>18</sup> S. Songkro, N. Rajatasereekul and N. Cheewasirungrueng, *World Acad. Sci. Eng. Technol.*, **55**, 113 (2009), <https://doi.org/10.5281/zenodo.1077062>

- <sup>19</sup> S. K. Lukman and S. Saidin, *J. Biomed. Mater. Res. Part A*, **108**, 1171 (2020), <https://doi.org/10.1002/jbm.a.36891>
- <sup>20</sup> M. J. R. Virlan, D. Miricescu, A. Totan, M. Greabu, C. Tanase *et al.*, *J. Chem.*, **2015**, 1 (2015), <https://doi.org/10.1155/2015/525832>
- <sup>21</sup> N. N. Saarani, J.-T. Kalitheerta, N. Shahab, H. Hermawan and S. Saidin, *Dent. Mater. J.*, **36**, 1 (2017), <https://doi.org/10.4012/dmj.2016-177>
- <sup>22</sup> N. S. V. Capanema, A. A. P. Mansur, A. C. de Jesus, S. M. Carvalho, L. C. de Oliveira *et al.*, *Int. J. Biol. Macromol.*, **106**, 1218 (2018), <https://doi.org/10.1016/j.ijbiomac.2017.08.124>
- <sup>23</sup> S. H. Park, H. S. Shin and S. N. Park, *Carbohydr. Polym.*, **200**, 341 (2018), <https://doi.org/10.1016/j.carbpol.2018.08.011>
- <sup>24</sup> O. Anjos, M. G. Campos, P. C. Ruiz and P. Antunes, *Food Chem.*, **169**, 218 (2015), <https://doi.org/10.1016/j.foodchem.2014.07.138>
- <sup>25</sup> M. A. Bonifacio, S. Cometa, A. Cochis, P. Gentile, A. M. Ferreira *et al.*, *Data Brief*, **20**, 831 (2018), <https://doi.org/10.1016/j.dib.2018.08.155>
- <sup>26</sup> L. Xia, N. Shrestha and B. Vemuri, in “Microbial Electrochemical Technology”, edited by S. V. Mohan, S. Varjani and A. Pandey, Elsevier, 2019, pp. 195-224
- <sup>27</sup> L. Chen, C. Yan and Z. Zheng, *Mater. Today*, **21**, 38 (2018), <https://doi.org/10.1016/j.mattod.2017.07.002>
- <sup>28</sup> K.-Y. Law, *J. Phys. Chem. Lett.*, **5**, 686 (2014), <https://doi.org/10.1021/jz402762h>
- <sup>29</sup> M. Ferrari, F. Cirisano and M. Morán, *Colloids Interfaces*, **3**, 1 (2019), <https://doi.org/10.3390/colloids3020048>
- <sup>30</sup> P. Perugini, I. Genta, B. Conti, T. Modena and F. Pavanetto, *Int. J. Pharm.*, **252**, 1 (2003), [https://doi.org/10.1016/s0378-5173\(02\)00602-6](https://doi.org/10.1016/s0378-5173(02)00602-6)
- <sup>31</sup> R. Machatschek and A. Lendlein, *J. Control. Release*, **319**, 276 (2020), <https://doi.org/10.1016/j.jconrel.2019.12.044>
- <sup>32</sup> D. Ahmad, I. van den Boogaert and J. Miller, *Energ. Sources Part A*, **40**, 2686 (2018), <https://doi.org/10.1080/15567036.2018.1511642>
- <sup>33</sup> M. A. Abd Jalil, A. R. Kasmuri and H. Hadi, *Skin Pharmacol. Physiol.*, **30**, 66 (2017), <https://doi.org/10.1159/000458416>
- <sup>34</sup> L. Tuksitha, Y. L. S. Chen and Y. L. Chen, *J. Asia-Pac. Entomol.*, **21**, 563 (2018), <https://doi.org/10.1016/j.aspen.2018.03.007>
- <sup>35</sup> P. C. Molan, in “New Strategies Combating Bacterial Infection”, edited by I. Ahmad and F. Aqil, Weinheim, Wiley VCH, 2009, pp. 229-253
- <sup>36</sup> J. Bertoneclj, U. Doberšek, M. Jamnik and T. Golob, *Food Chem.*, **105**, 822 (2007), <https://doi.org/10.1016/j.foodchem.2007.01.060>
- <sup>37</sup> R. Yaghoobi, A. Kazerouni and O. Kazerouni, *Jundishapur J. Nat. Pharm. Prod.*, **8**, 100 (2013), <https://doi.org/10.17795/jjnpp-9487>
- <sup>38</sup> S. Samarghandian, T. Farkhondeh and F. Samini, *Pharmacog. Res.*, **9**, 121 (2017), <https://doi.org/10.4103/0974-8490.204647>
- <sup>39</sup> A. Henriques, S. Jackson, R. Cooper and N. Burton, *J. Antimicrob. Chemother.*, **58**, 773 (2006), <https://doi.org/10.1093/jac/dk1336>